forests

MDPI

Article

Nocturnal Water Use Partitioning and Its Environmental and Stomatal Control Mechanism in *Caragana korshinskii* Kom in a Semi-Arid Region of Northern China

Wei Li [1,2], Yu Zhang [3,4,5,*], Nan Wang [1], Chen Liang [1,2], Baoni Xie [1,2], Zhanfei Qin [1,2], Ying Yuan [6] and Jiansheng Cao [7,*]

1 School of Land Science and Space Planning, Hebei GEO University, Shijiazhuang 050031, China; weil87land@hgu.edu.cn (W.L.); wn305099@163.com (N.W.); liangchen214@mails.ucas.ac.cn (C.L.); xbn-feya@nwafu.edu.cn (B.X.); zhanfeiqin@163.com (Z.Q.)
2 International Science and Technology Cooperation Base of Hebei Province: Hebei International Joint Research Center for Remote Sensing of Agricultural Drought Monitoring, Hebei GEO University, Shijiazhuang 050031, China
3 School of Geographical Sciences, Hebei Normal University, Shijiazhuang 050024, China
4 Hebei Key Laboratory of Environmental Change and Ecological Construction, Shijiazhuang 050024, China
5 Hebei Technology Innovation Center for Remote Sensing Identification of Environmental Change, Shijiazhuang 050024, China
6 School of Urban Geology and Engineering, Hebei GEO University, Shijiazhuang 050031, China; yuanyingson@hgu.edu.cn
7 Center for Agricultural Resources Research, Institute of Genetics and Developmental Biology, Chinese Academy of Sciences, Shijiazhuang 050022, China
* Correspondence: yuzhang89@bnu.edu.cn (Y.Z.); caojs@sjziam.ac.cn (J.C.)

Abstract: As an important aspect of plant water consumption, nocturnal water use (E_n) behavior provides reliable information on the effect of plantation carbon and water budgets at stand and regional scales. Therefore, quantifying E_n and its environmental and stomatal controlling mechanisms is urgent to establish adaptation strategies for plantation management in semiarid regions. With the help of the sap flow technique, our study investigated the seasonal variations in canopy transpiration and canopy conductance in a *Caragana korshinskii* Kom plantation. Environmental variables were measured concurrently during the growing seasons of 2020 and 2021. The results indicated that the average E_n values were 0.10 mm d^{-1} and 0.09 mm d^{-1}, which accounted for 14% and 13% of daily water use, respectively, over two years. The proportions of nocturnal transpiration (T_n) to E_n were approximately 49.76% and 54.44%, while stem refilling (R_e) accounted for 50.24% and 45.56% of E_n in 2020 and 2021, respectively, indicating that *C. korshinskii* was able to draw on stored stem water to support transpiration. E_n was predominantly affected by nocturnal canopy conductance (G_{c-n}), air temperature (T_{a-n}) and wind speed (u_{2-n}). In contrast, G_{c-n} and T_{a-n} explained the highest variation in T_n and nocturnal vapor pressure (VPD_n), and u_{2-n} explained the highest variation in R_e. Total effects of the five environmental and stomatal variables explained 50%, 36% and 32% of E_n, T_n and R_e variation, respectively. These findings could enable a better understanding of nocturnal water use dynamics and their allocation patterns in *C. korshinskii* plantations on the Bashang Plateau. Moreover, our results reveal the water use strategies of artificial shrubs and highlight the importance of incorporating nocturnal water use processes into large-scale ecohydrological models in semiarid regions.

Keywords: nocturnal water use; nocturnal transpiration; stem refilling; canopy stomatal conductance; *Caragana korshinskii* Kom

Citation: Li, W.; Zhang, Y.; Wang, N.; Liang, C.; Xie, B.; Qin, Z.; Yuan, Y.; Cao, J. Nocturnal Water Use Partitioning and Its Environmental and Stomatal Control Mechanism in *Caragana korshinskii* Kom in a Semi-Arid Region of Northern China. *Forests* **2023**, *14*, 2154. https://doi.org/10.3390/f14112154

Academic Editor: Cate Macinnis-Ng

Received: 19 June 2023
Revised: 23 October 2023
Accepted: 26 October 2023
Published: 30 October 2023

1. Introduction

Nocturnal water use is defined as the sap flux dynamics that occur at night with incomplete stomatal closure, and is different to diurnal water use in a single component.

During the past two decades, nocturnal water use has been reported across a range of forest species and habitats; and the average contribution of nocturnal water use to daily water use is approximately 12% in diverse woody species, and reaches up to 30–60% in water-limited environments [1–5]. The occurrence, pattern and alteration of nocturnal water use play important roles in adjusting predawn disequilibrium between leaves and soil [6], reducing hydraulic redistribution within dry rhizosphere soils [7], avoiding the delay between carbon assimilation and stomatal opening in the early morning hours [8,9] and facilitating oxygen and nutrient uptake for tree growth [10,11]. Therefore, nocturnal water use is regarded as a special water use strategy that enables plants to adapt to different environments, and the accurate quantification of nocturnal water use and its contribution to total daily water use is important for understanding the carbon and water budgets of forest ecosystems [12]. However, there is limited research on the nocturnal water use behavior of planted shrubs in arid and semiarid regions, which limits our understanding of the water use strategy of shrubs, and of future changes in ecosystem function in these regions.

Nocturnal water use can be characterized as nocturnal transpiration from leaves and the water required for stem refilling, separately or synergistically [13–15]. Nocturnal transpiration is driven by leaf-to-air vapor pressure differences under the influence of nocturnal stomatal openness. It might help to promote nutrient absorption via the mass flow of water and carbon fixation in the early morning [16]. Stem refilling is an effective type of internal water storage, that functions to replenish the large amount of water consumed during diurnal transpiration. Water absorption by the roots during the night is needed to overcome xylem and stem water deficits that occur in the daytime. Precisely identifying nocturnal transpiration and stem refilling components from continuous nocturnal water use will contribute to developing a better understanding of physiological responses to external environmental changes. Several methods have been proposed to distinguish nocturnal transpiration and stem refilling from nocturnal water use, such as the Penman–Monteith model [17], a flow model based on a resistance network [18], a time series model with one or more exogenous inputs [19,20] and a forecasted refilling method regarding determination-based vapor pressure deficits (*VPD*) [13,21]. The forecasted refilling method, conducted by analyzing the slope of a daily sap flux curve, has been proven to be a simple and useful fraction method, and has been successfully applied on rainless nights in natural [1,2], planted [22,23] and urban forests [5].

The reported crucial environmental drivers of nocturnal water use include nocturnal VPD, temperature, wind speed and soil water content [7,22,24]. High nocturnal water use usually occurs when air temperatures and soil water content are high. Additionally, nocturnal water use in response to environmental factors is achieved through adjustments to nocturnal stomatal conductance. High nocturnal water use is regularly associated with high nocturnal stomatal conductance, which tracks VPD-induced variations in stomatal apertures [25]. The environmental and stomatal control mechanisms of nocturnal transpiration and stem refilling are generally different, according to prior studies. The concurrent occurrence of stomatal openness and vapor pressure differences between the atmosphere and leaf surface provide the necessary conditions for nocturnal transpiration [5]. Therefore, nocturnal transpiration is usually positively correlated with VPD and wind speed, while stem refilling is commonly correlated to biological and physiological variations, such as plant size, anatomical features, plant water status, etc. [26]. However, similar stem refilling proportion results were reported for plants of the same species but different individual sizes in planted forests in Mexico [27]. Therefore, the environmental and stomatal mechanism of nocturnal water use is still uncertain, and a more advanced understanding of the total effect of concurrent environmental and stomatal controls on nocturnal water use and its fractions is needed.

As a typical shrub type in arid and semiarid regions, *Caragana korshinskii* Kom has commonly been used since the implementation of the Beijing–Tianjin Sand Source Restoration Project in 2000 for establishing protective shrub plantations on the Bashang Plateau. Due to their strong drought tolerance, *C. korshinskii* plantations play an important role in

windbreak and sand fixation, soil and water conservation, soil restoration and ecological protection. Major research has been conducted on *C. korshinskii* plantations to understand their daily water use and their capacity to adapt to water-limited environmental conditions [28–30]. However, the ecological importance of nocturnal water use dynamics in *C. korshinskii* plantations is poorly understood, and under soil water scarcity the responses of nocturnal water use, nocturnal transpiration and stem refilling to concurrent environmental and stomatal variables remain fully unknown. Therefore, we hypothesize that (1) nocturnal water use occurs in *C. korshinskii* plantations and has a great impact on daily water loss; (2) the environmental and stomatal controls of nocturnal water use and its fractions (nocturnal transpiration and stem refilling) may be subject to different influences. The objectives of this study are as follows: (1) to analyze the nocturnal water use dynamic and its contribution to the daily water use of *C. korshinskii*, (2) to determine the allocation of the nocturnal transpiration and stem refilling of *C. korshinskii* and (3) to explore the total effects of concurrent environmental and stomatal controls on nocturnal water use, nocturnal transpiration and stem refilling.

2. Materials and Methods

2.1. Site Description

The research area is situated at the northern Bashang Plateau, Kangbao County, which belongs to the northwest of the Beijing–Tianjin–Hebei Region of China (Figure 1). The climate of the region is arid and cold with mean annual precipitation of 330.0 mm and mean annual temperature of 2.3 °C (1980–2020). However, the potential evapotranspiration is over 850 mm. The mean annual wind speed is 3.15 m s^{-1}. The field site located at the Kangbao pasture region (114°48′ E, 42°07′ N, altitude 1305 m) is composed of planted forests of pure *C. korshinskii*, which were planted according to the Beijing–Tianjin Sandstorm Source Sontrol Project. The *C. korshinskii* plantation is about 20 years old, with an average height of 179.28 ± 30.74 cm and stem basal diameter at stem base (10–15 cm above the ground) of 2.38 cm. The soil is mainly sandy loam with a high sand content of 52.89% and low clay content of 7.86% [31].

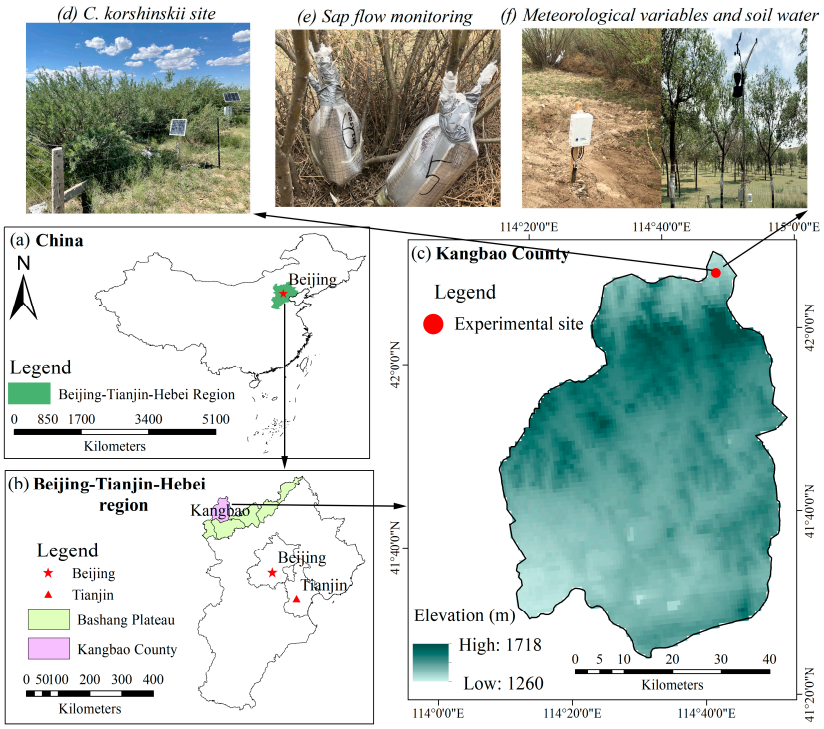

Figure 1. Geographical research sites in this study, including (**a**–**c**) Beijing–Tianjin–Hebei region and the Bashang Plateau of Hebei province, (**d**) *Caragana korshinskii* Kom site in Kangbao County, (**e**,**f**) sap flow measurement and meteorological variables, soil water monitoring.

2.2. Materials and Experimental Design

2.2.1. Materials

We selected a sample site for the study and established a 20 m × 20 m fenced enclosure for purposes of monitoring. Based on the distribution of stem base diameter (SBD), nine sample stems (SDB = 2.68, 2.96, 3.38, 3.62, 3.66, 3.76, 4.14, 4.24 and 4.38 cm) of healthy and non-stressed *C. korshinskii* were selected for the 2020 and 2021 experimental periods. We assumed that the whole cross-section of these stems in *C. korshinskii* were conductive, sapwood area (A_s) which was then estimated as a stem basal cross-sectional area. The total sapwood area in the experimental plot was 6877.70 cm^2.

2.2.2. Environmental Variables

Meteorological parameters were measuring at a height of 2 m in a nearby clear space with an Onset HOBO U21 automatic weather station (Onset Computer Corp., Bourne, MA, USA) and included the following: photosynthetically active radiation (*PAR*, μmol m^{-2} s^{-1}), air temperature (T_a, °C), relative humidity (*RH*, %), wind speed (u_2, m s^{-1}) and precipitation (*P*, mm). Vapor pressure deficits (*VPD*, kPa) were calculated from T_a and *RH* according to Campbell and Norman [32]. These meteorological data were available as 10 min averages from 30 s samples and stored using CR1000 data loggers (Campbell Scientific, Logan, UT, USA).

The soil water content (*SWC*, m^{-3} m^{-3}) was measured at five depths (i.e., 5, 15, 30, 50, 80 cm) with an EC-5TE sensor (Decagon, Inc. Pullman, WA, USA) and recorded at 30 min internals by CR1000 data loggers (Campbell Scientific, Logan, UT, USA).

Relative extractable soil water content (*REW*) was calculated using averaged *SWC* across 0–100 cm:

$$REW = \frac{SWC - SWC_{min}}{SWC_{max} - SWC_{min}}$$

where SWC_{min} and SWC_{max} are the minimum and maximum daily average soil water content, respectively, during the two whole years.

2.2.3. Sap Flow Measurements

We measured xylem sap flux on stems using thermal dissipation probes (TDPs) during two growing seasons in 2020 and 2021 (1 May to 30 September). Nine pairs of Granier-type probes (TDP10, Dynamax Inc., Houston, TX, USA) consisting of a copper-constantan thermojunction were inserted at a depth of 10 mm into the xylem sapwood of stems of nine shrubs at a height of 40 cm above the ground on the northern side. In order to protect the probes to reduce solar heating and extraneous thermal gradients, an aluminum foil shield wrap was applied for each pair of Granier-type probes. Thermal insulation cotton and aluminum foil were placed on the ground around the probe to reduce the influence of ground temperature on its measurements. Additionally, for the homogenous and dense plantation stands, the influences of natural thermal gradients on sap flow measurements could be assumed to be negligible [22,33]. The detail procedure for measuring sap flow velocity can be found in [31]. The sap flow velocity (*SF*, mL cm^{-2} min^{-1}) could be calculated from the measured temperature difference at 30 min intervals (CR1000, Campbell Scientific Inc., Logan, UT, USA) according to Granier [34]:

$$SF = 0.0119 \times \left((\Delta T_{max} - \Delta T) / \Delta T \right)^{1.231} * 60$$

$$E = \overline{SF} \times \left(A_{si} / A_g \right) \times 600$$

where ΔT (°C) is the temperature difference between the two probes at any given time, and ΔT_{max} (°C) is the maximum temperature difference between sensors, which was determined as the maximum value of daily ΔT_{max} over a 9-day period to avoid underestimation of the nighttime sap flow. (1) A linear regression of local maximal ΔT_{max} determined by a 9-day moving window and time (day) was performed and local ΔT_{max} values below the linear regression line were eliminated; (2) A new linear regression was then made based

on the remaining ΔT_{max} points; (3) finally the "real ΔT_{max}" was recalculated by the new linear regressions [35,36]. As there was only one probe per sample stem, the azimuthal and radial variation in sap flow velocity were not taken into account in this study. We assume that these variations were low [23,37]. E is canopy transpiration per area of ground (mm h^{-1}); $\overline{SF}$ is the average sap flow velocity of sampled shrubs (ml cm^{-2} min^{-1}), A_g is the ground surface area of the studied plots (400 m^2), and A_{si} is the total sapwood area in the studied plot.

Daily SF and E were further divided into diurnal SF/E (SF_d/E_d) and nocturnal SF/E (SF_n/E_n) based on the value of PAR. Diurnal SF_d/E_d was defined as a PAR value greater than 5 µmol m^{-2} s^{-1}, while nocturnal SF_n/E_n was correspondingly defined as a PAR value less than 5 µmol m^{-2} s^{-1} or equal to 0. Therefore, nocturnal SF_n/E_n ranged from 19:30 to 4:30 in May, 20:00 to 4:30 in June, 20:00 to 4:30 in July, 19:00 to 5:00 in August, 18:30 to 5:30 in September during the growing season in 2020 (Figure 2a). In 2021, nocturnal SF_n/E_n ranged from 19:30 to 4:30 in May, 20:00 to 4:00 in June, 19:00 to 4:30 in July, 19:30 to 5:00 in August and 18:30 to 5:30 in September during the growing season (Figure 2b). To differentiate between the contributions of nocturnal transpiration (T_n) and stem refilling (R_e) to SF_n, the forecasted refilling method was used [2,21]. Fisher et al. [21] suggested that if no nocturnal water loss occurred, SF_n would gradually continue to fall to zero flow via an exponential decay function. However, we found that SF_n was greater than zero flow during the whole growing season in 2020 and 2021, and decreased at the beginning of the night but then increased until sunrise (Figure 2). It was indicated that the early sloped phase of SF_n mostly consisted of R_e and a nonzero linear phase representing T_n later [2,38]. Therefore, an exponential relationship between SF_n and VPD_n was conducted to fit the first 3 to 5 h:

$$SF_n = a \times \exp(b \times VPD_n)$$

where a and b are fitting parameters. The relationship between SF_n and VPD_n was determined, with R^2 consistently > 0.96 (Figure A1) during the growing season in 2020. This approach was only applied for every clear night with low nocturnal VPD, so that: (1) the area below the forecasting curve could be considered as sap flow caused by R_e, due to lack of strong atmospheric demand for nocturnal water loss; (2) the area above the curve could be considered as sap flow caused by T_n.

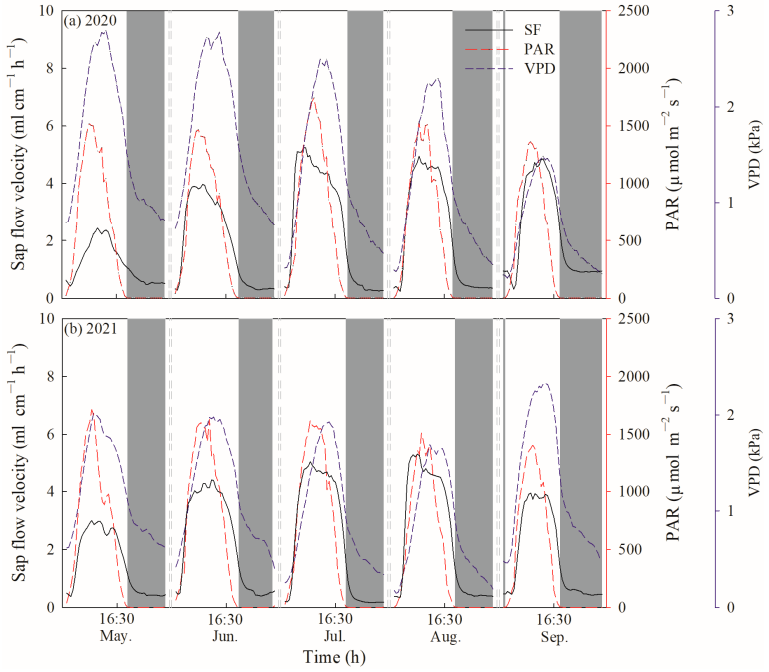

Figure 2. Hourly variations in sap flow velocity of *C. korshinskii*, photosynthetically active radiation and vapor pressure deficits.

2.2.4. Canopy Conductance

Since the distribution of the *C. korshinskii* plantation was relative uniform and the canopy was not closed (the largest value of leaf area indices was 0.43 m^2 m^{-2}), the canopy was well-coupled to the atmosphere [31], The canopy conductance can be calculated by the simplified Penman–Monteith equation [39] using the following formula:

$$G_c = \gamma \lambda E / \rho C_p VPD$$

where G_c is canopy conductance (mm s^{-1}), γ is the psychometric constant (kPa, $°C^{-1}$), λ is latent heat of water vaporization (MJ kg^{-1}), ρ is the air density (kg m^{-3}) and C_p is the specific heat of the air (MJ kg^{-1} $°C^{-1}$).

Nocturnal G_c (G_{c-n}) were also defined as stomatal opening occurring when a *PAR* value was less than 5 μmol m^{-2} s^{-1}.

2.3. Data Analysis

The differences in the environmental and stomatal variables during the two growing seasons of 2020 and 2021 were tested using a paired-samples *t*-test. Significant differences in E_n, T_n and R_e among different months during the growing season were tested using one-way ANOVA at a significance level of $\alpha = 0.05$. Pearson's correlation coefficient and a partial correlation coefficient were used to estimate associated pairwise relationships between $E_n/T_n/R_e$ and all environmental and stomatal variables. Then, linear, polynomial and nonlinear (i.e., exponential growth function, exponential threshold function) regression analyses were conducted to investigate the relationships between $E_n/T_n/R_e$ and major environmental and stomatal variables (i.e., VPD_n, $u_{2\text{-}n}$, T_{a-n} and G_{c-n}). However, these single-variable relationships above might be weak and showed a high degree of scatter, which was due to a strong effect of certain other factors. Therefore, an upper boundary line method was applied to determine these single-variable relationships of $E_n/T_n/R_e$ and VPD_n, $u_{2\text{-}n}$, T_{a-n} and G_{c-n}, without interference from other factors. The study divided VPD_n, $u_{2\text{-}n}$, $T_{a\text{-}n}$ and $G_{c\text{-}n}$ into several segments, with intervals of segments of VPD_n, $u_{2\text{-}n}$, T_{a-n} and G_{c-n} of 0.5 kPa, 1 m s^{-1}, 5 °C and 0.5 mm s^{-1}, respectively. Then, an upper boundary line was conducted as suitable linear and nonlinear functional forms based on the data of $E_n/T_n/R_e$ of at least one standard deviation greater than the mean $E_n/T_n/R_e$ at each VPD_n, $u_{2\text{-}n}$, T_{a-n} and G_{c-n} interval. All statistical analyses were conducted using SPSS 21.0 (SPSS Inc., Chicago, IL, USA) and all figures were created using Sigmaplot 11.0 software (Hearne Scientific Software Plc, Melbourne, Australia).

A path coefficient model was developed to quantify the direct and indirect effects of environmental and stomatal variables on E_n, T_n and R_e, respectively. The initial model included all potential paths according to current knowledge and the above linear/nonlinear analyses. (1) VPD_n, $u_{2\text{-}n}$, T_{a-n}, *REW* and G_{c-n} were considered to directly affect E_n, T_n and R_e, respectively. Daily *REW* was used to respond to $E_n/T_n/R_e$ since there was no significant difference between diurnal and nocturnal *REW* in this study. (2) $u_{2\text{-}n}$ may affect $E_n/T_n/R_e$ by altering VPD_n, which may also affect $E_n/T_n/R_e$ by altering G_{c-n}. *REW* may affect $E_n/T_n/R_e$ by adjusting nocturnal canopy conductance. The standardized path coefficients were calculated through the maximum likelihood method. Path analysis was conducted using AMOS 22.0 (SPSS Inc., Chicago, IL, USA).

3. Results

3.1. Environmental Conditions

The average diurnal photosynthetically active radiation (*PAR*) values were 681.16 ± 201.18 μmol m^{-2} s^{-1} and 744.18 ± 200.69 μmol m^{-2} s^{-1} during the growing season in 2020 and 2021, respectively. The averaged nocturnal weed speeds ($u_{2\text{-}n}$) were 0.76 ± 0.67 m s^{-1} and 0.80 ± 0.75 m s^{-1} during the night in 2020 and 2021, respectively (Figure 3a). Nocturnal air temperature (T_{a-n}) displayed marked seasonal variations, with ranges of 2.04 to 22.40 °C and −1.89 to 22.61 °C, and mean values of 13.79 ± 4.38 °C and 13.93 ± 4.56 °C in

2020 and 2021, respectively. The average nocturnal vapor pressure deficits (VPD_n) were 0.60 ± 0.34 kPa and 0.62 ± 0.31 kPa during the growing season in 2020 and 2021, respectively (Figure 3b). A significant difference was observed in *REW* between 2020 and 2021 (F = 22.299, $p < 0.000$). The daily *REW* ranged from 0.31 to 0.79 and 0.31 to 0.98, with mean values of 0.42 ± 0.11 and 0.46 ± 0.16, in 2020 and 2021, respectively (Figure 3c).

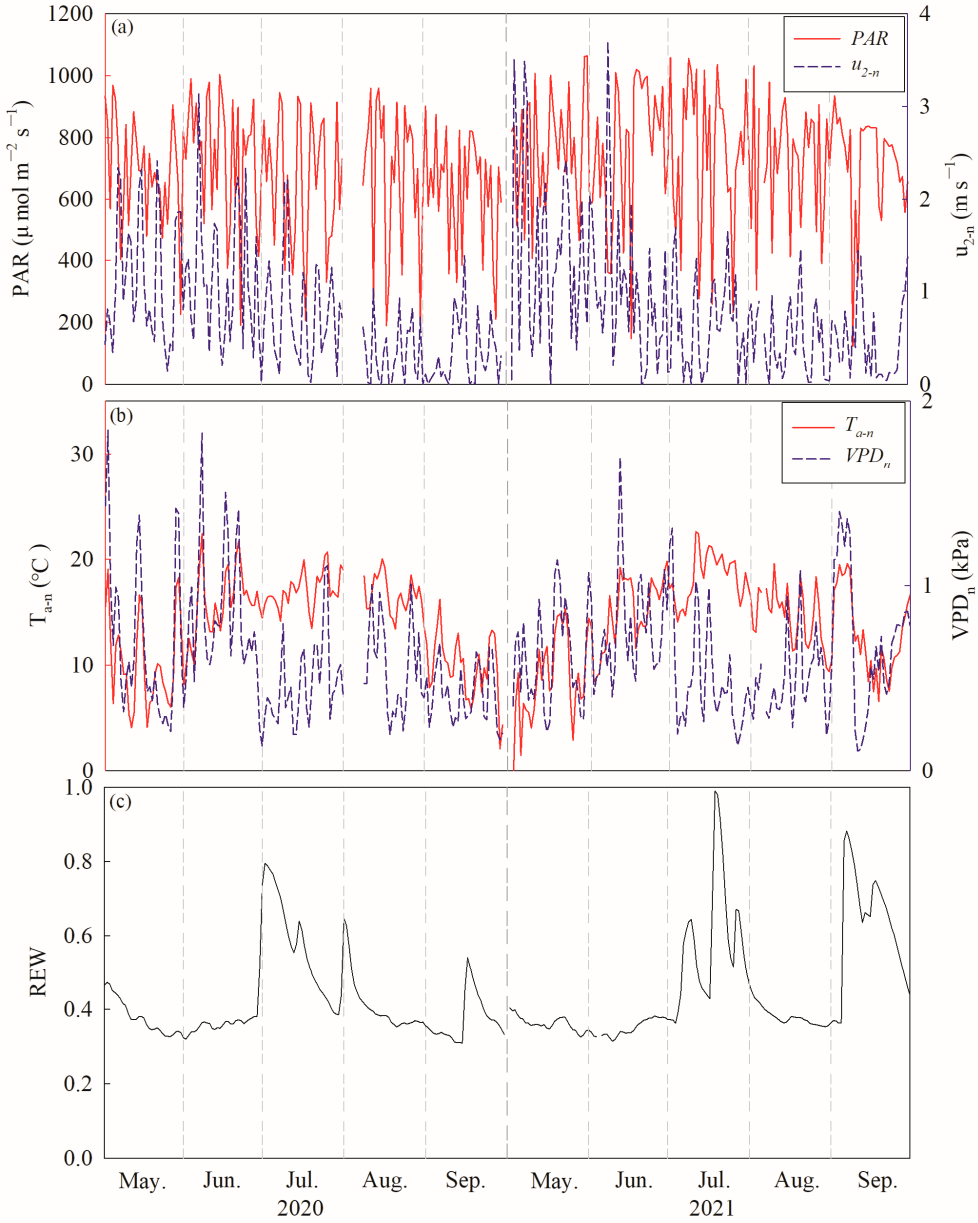

Figure 3. Diurnal variations of (**a**) photosynthetically active radiation (*PAR*) and nocturnal wind speed at the height of 2 m ($u_{2\text{-}n}$), (**b**) nocturnal air temperature ($T_{a\text{-}n}$) and nocturnal vapor pressure deficits and (VPD_n) (**c**) soil water content at a depth 0–100 cm (*REW*) in 2020 and 2021.

3.2. Variations in Nocturnal Water Use

The annual average E_d values for *C. korshinskii* were 0.64 ± 0.24 mm d^{-1} and 0.69 ± 0.23 mm d^{-1}; meanwhile, the accumulated E_d values over the growing season were 92.51 mm and 103.26 mm in 2020 and 2021, respectively. While the E_n values ranged from 0.01 to 0.61 mm d^{-1} in 2020, with a mean value of 0.10 ± 0.08 mm d^{-1}, whereas in 2021, E_n ranged from 0.01 to 0.59 mm d^{-1} with a mean value of 0.09 ± 0.07 mm d^{-1}. The accumulated E_n values over the growing season were 14.36 mm and 14.51 mm in 2020 and 2021, respectively, accounting for 15.48% and 14.04% of the accumulated diurnal water

use and 13.40% and 12.31% of the accumulated daily water use over the same period. The annual average E_n:E_d values were 0.18 ± 0.15 and 0.17 ± 0.17, whereas the E_n:E values were 0.14 ± 0.09 and 0.13 ± 0.10 in 2020 and 2021, respectively (Figure 4a,b). No significant difference was observed for either E_n:E_d or E_n:E between 2020 and 2021; however, in both years, E_n:E_d and E_n:E were significantly higher in May and September than from June to August ($p < 0.000$, ANOVA).

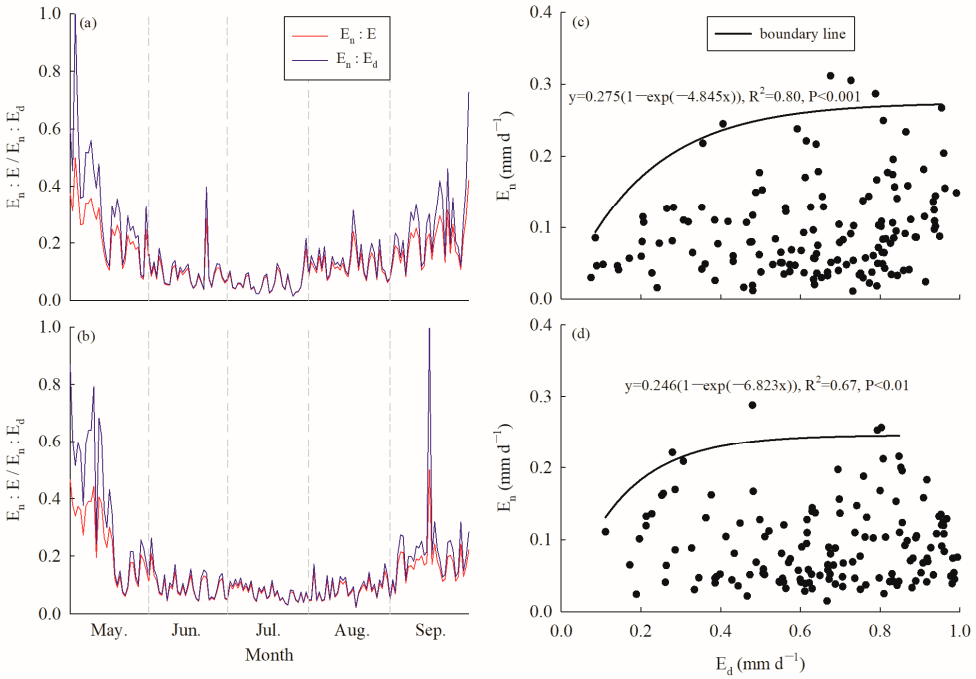

Figure 4. Variation in the ratio of nocturnal to diurnal (E_n:E_d, red line) and nocturnal to daily water use (E_n:E, blue line) in (**a**) 2020 and (**b**) 2021; the relationship between E_n and E_d (black solid circle) and boundary line analysis (black line) in (**c**) 2020 and (**d**) 2021.

The saturated exponential analysis showed a significant positive relationship between E_n and E_d, but the goodness of fit was better in 2020 (R^2 = 0.80) than in 2021 (R^2 = 0.67) after conducting boundary line analysis (Figure 4c,d). E_n increased with increasing E_d, while it tended to be saturated when E_d reached approximately 0.4–0.5 mm d^{-1} in 2020 and 0.4 mm d^{-1} in 2021.

3.3. Components of Nocturnal Transpiration and Xylem Refilling

T_n was low and stable before mid-August, while it showed an obvious peak that appeared in mid-September; however, R_e was relatively higher in May and remained stable between June and September in 2020 ($p < 0.000$, ANOVA) (Figure 5a and Table 1). In 2021, T_n was low and stable between July and August, but showed peaks in early May and mid-September; however, R_e in May and July was significantly lower than that in June and August ($p < 0.000$, ANOVA) and showed a peak in early September (Figure 5b and Table 1). The annual average T_n values were 0.049 ± 0.073 and 0.052 ± 0.068 mm d^{-1}, while the R_e values were 0.050 ± 0.038 and 0.043 ± 0.030 mm d^{-1} in 2020 and 2021, respectively. The accumulated T_n values over the growing season were 7.14 and 7.90 mm in 2020 and 2021, respectively, accounting for 49.76% and 54.44% of E_n. Meanwhile, the sums of R_e were 7.22 and 6.61 mm, accounting for 50.24% and 45.56% of E_n in 2020 and 2021, respectively.

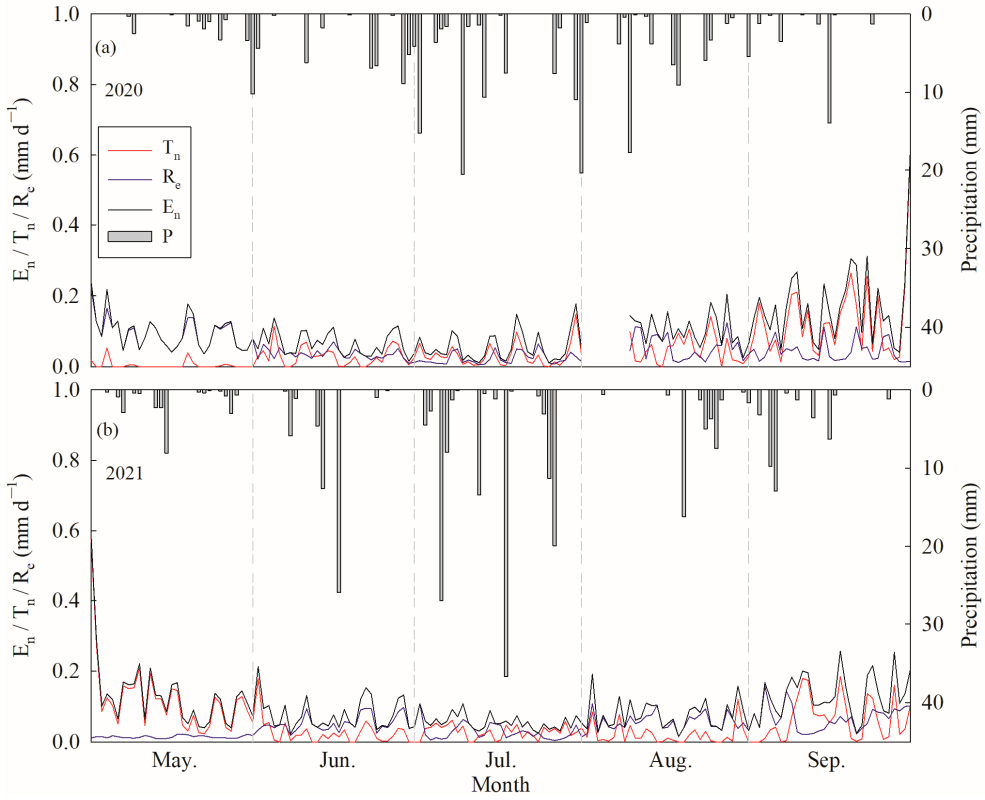

Figure 5. Daily variations of nocturnal water use (E_n), nighttime canopy transpiration (T_n) and stem refilling (R_e) and the distribution of precipitation during the growing season in (**a**) 2020 and (**b**) 2021.

Table 1. Seasonal variation in nocturnal water use (E_n), nocturnal transpiration (T_n), stem refilling (R_e) and contribution of T_n and R_e to E_n (T_n:E_n and R_e:E_n) during the growing season from May to September of 2020 and 2021 for *Caragana korshinskii* Kom.

	Month	E_n (mm)	T_n (mm)	R_e (mm)	T_n:E_n (%)	R_e:E_n (%)
2020	May	3.05	0.14	2.91	4.72	95.28
	June	1.95	0.89	1.05	45.86	54.14
	July	1.73	1.00	0.73	57.91	42.09
	August	2.39	1.14	1.25	47.69	52.31
	September	5.24	3.97	1.28	75.68	24.32
2021	May	4.12	3.68	0.44	89.32	10.68
	June	2.32	0.76	1.56	32.64	67.36
	July	1.74	0.89	0.85	50.96	49.04
	August	2.34	0.61	1.73	26.07	73.93
	September	3.99	1.96	2.02	49.25	50.75

3.4. Environmental and Stomatal Drivers of Nocturnal Water Use

The statistical analysis indicated that the significance effects of the environmental and stomatal variables on E_n had a ranking of $G_{c-n} > u_{2-n} > T_{a-n} > PAR > RH_n$ in 2020 and $G_{c-n} > T_{a-n} > RH_n > PAR > u_{2-n}$ in 2021. Moreover, T_n was positively correlated with G_{c-n} and PAR, but negatively correlated to T_{a-n}, u_{2-n} and VPD_n in 2020; while it was positively correlated with G_{c-n}, and negatively correlated to T_{a-n}, RH_n and VPD_n in 2021, when controlling for R_e. However, R_e was positively correlated with PAR and VPD_n in both years, but negatively to RH_n and T_{a-n} in 2020 and to RH_n and u_{2-n} in 2021, when controlling for T_n (Table 2).

Table 2. Correlation and partial correlation coefficients between nocturnal water use (E_n, T_n and R_e) and environmental, stomatal variables for *C. korshinskii* in 2020 and 2021.

	Controlling Variable	Biological Variables					
		PAR	T_{a-n}	RH_n	u_{2-n}	VPD_n	G_{c-n}
2020	E_n	0.455 **	−0.496 **	−0.183 **	−0.532 **	-	0.748 **
	Sig	0.00	0.00	0.03	0.00	-	0.00
	T_n	0.183	−0.455	-	−0.414	−0.284	0.746
	Sig	0.02	0.00	-	0.00	0.00	0.00
	R_e	0.458	−0.332	−0.543	-	0.366	-
	Sig	0.00	0.00	0.00	-	0.00	-
2021	E_n	0.214 **	−0.459 **	−0.262 **	−0.169 *	-	0.658 **
	Sig	0.00	0.00	0.00	0.04	-	0.00
	T_n	-	−0.599	−0.234	-	−0.156	0.529
	Sig	-	0.00	0.00	-	0.05	0.00
	R_e	0.285	-	−0.313	−0.375	0.440	-
	Sig	0.00	-	0.00	0.00	0.00	-

Note: *PAR* = photosynthetically active radiation; T_{a-n} = nocturnal air temperature; RH_n = nocturnal relative humidity; u_{2-n} = nocturnal wind speed; VPD_n = nocturnal vapor pressure deficits; G_{c-n} = nocturnal canopy stomatal conductance; ** indicates $p < 0.01$, * indicates $p < 0.05$.

Both E_n and T_n decreased linearly with increasing T_{a-n}, which explained 87% and 99% of the variation in E_n, and 60% and 84% of the variation in T_n, during the measurement periods of 2020 and 2021, respectively. Meanwhile, R_e was stable and decreased slightly with increasing T_{a-n} in 2020, and increased linearly with increasing T_{a-n} in 2021 (Figure 6a–c). Both E_n and T_n displayed an exponential decay response to VPD_n, but the goodness of fit was better (R^2 = 0.72, 0.93) in 2020 than in 2021 (R^2 = 0.78, 0.63). Meanwhile, R_e exhibited a polynomial response to VPD_n and tended to fall off when VPD_n > 1.0 kPa in 2020, but increased linearly with increasing VPD_n (Figure 6d–f). u_{2-n} explained 90%, 87% and 91% of the variation in E_n, T_n and R_e in 2020, and 47%, 32% and 93% in 2021, following exponential decay functions, respectively (Figure 6g–i). E_n exhibited an exponential saturation response to G_{c-n} both in 2020 and 2021, and E_n tended to level off at 1.5 mm s^{-1} in 2021. T_n increased linearly with increasing G_{c-n} in 2020, but had an exponential saturation response to G_{c-n} in 2021. Meanwhile, R_e remained stable with different G_{c-n} values in 2020, but had an exponential decay response to G_{c-n} in 2021 (Figure 6j–l).

Combined with the direct and indirect effects, VPD_n positively affected E_n (0.146) and R_e (0.476), while it negatively affected T_n (−0.135). u_{2-n} decreased E_n (−0.157) and R_e (−0.273) during two growing seasons. Finally, the total effect of these five environmental and stomatal variables explained 50%, 36% and 32% of the variation in E_n, T_n and R_e, respectively (Figure 7).

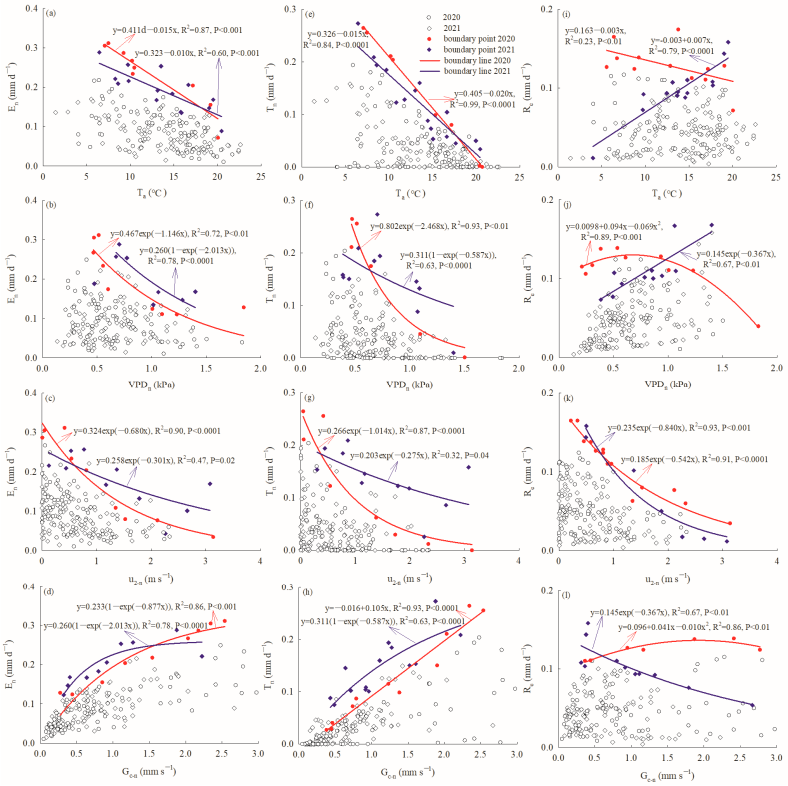

Figure 6. Nocturnal water use (E_n) relationship with (**a**) nocturnal air temperature, (**b**) nocturnal vapor pressure deficits, (**c**) nocturnal weed speed, (**d**) nocturnal canopy conductance; nocturnal transpiration (T_n) relationship with (**e**) nocturnal air temperature, (**f**) nocturnal vapor pressure deficit, (**g**) nocturnal weed speed, (**h**) nocturnal canopy conductance; stem refilling (R_e) relationship with (**i**) nocturnal air temperature, (**j**) nocturnal vapor pressure deficit, (**k**) nocturnal weed speed, (**l**) nocturnal canopy conductance.

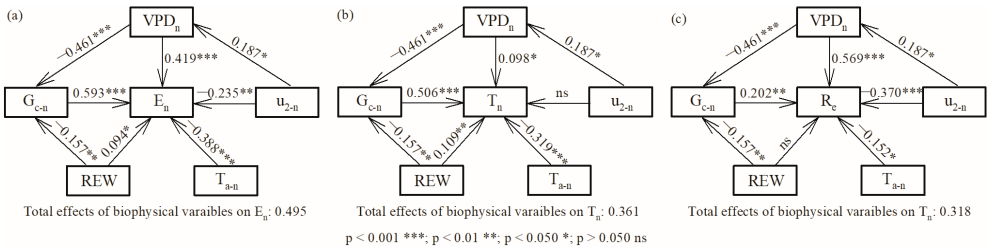

Figure 7. Direct and indirect effects of environmental and stomatal variables on (**a**) nocturnal water use, (**b**) nocturnal transpiration, and (**c**) stem refilling in 2020 and 2021.

4. Discussion

4.1. The Application of Thermal Dissipation Probes for C. korshinskii Plantation

Sap flow was usually measured using the stem heat balance method for shrubs with short height and small diameter at breast height (DBH) [28]. However, in arid and semiarid regions, the influence of high wind and strong solar radiation brought great challenges to the complete sap flow velocity data continuity and stability. The thermal dissipation probes (TDP10) method has recently been used to measure the sap flow velocity for plants with small DBH, such as bamboo species [40], *Populus adenopoda* [41], *Aegiceras corniculatum* [42] and so on. Compared with an induced hydraulic pressure and sap flow changing device and a whole-culm pot weighing method, the 10 mm long TDP was proven to be a valid means of measuring the sap flow of *Phyllostachys pubescens* [43]. Additionally, an environmental temperature reduction from 25 to 0 °C did not alter the values of ΔT_{max} between a heated probe and a reference probe when there was no sap flow, verifying that ΔT measured at

night can be used as a reference in daytime [44]. The daily average temperature in our study was 15.14 ± 3.88 °C and 15.02 ± 4.28 °C during the growing season in 2020 and 2021, respectively (Figure 3b). Therefore, TDP10 could be verified to be a valid means of accurately quantifying the water use of *C. korshinskii* with SDB less than 5 cm in this study.

4.2. Nocturnal Water Use Behaviors of C. korshinskii

Increasing evidence from leaf microstructure and gas exchange experiments has suggested that stomata are partially open throughout the night, which provides the necessary conditions for nocturnal water use [5,38]. Like other tree and shrub species, such as *P. euphratica*, *P. tabuliformis*, *A. truncatum*, *S. superba*, *Q. lancifolia*, *A. latifolia*, *A. jorullensis*, *S. psammophila*, we observed substantial *C. korshinskii* E_n at night during the growing seasons in 2020 and 2021 (Figure 2). We found that the water stored in the stems, refilled mostly during the night from soil water uptake through the roots, is usually used for supply water consumption during the daytime [23,45]. However, the E_n of *C. korshinskii* was much lower than that reported in plant species in the past. This may be related to the smaller daily transpiration of *C. korshinskii* plantations and the lower soil water content (Figure 3c) on the Bashang Plateau [31]. The E_n:E values in this study were 14% and 13% in 2020 and 2021, respectively, which were similar to the values reported for *P. tabuliformis* and *A. truncatum* [22]. The sharp increase in E_n:E at the beginning and the end of the growing season in both 2020 and 2021 was similar to that found in birch [45] and a *P. tomentosa plantation* [23]. Nocturnal water loss was more important under drought conditions than in other conditions [15]. The sharp increase in sap flow during the early growth stage had a function of refilling xylem conduits that accumulated embolisms during winter in the previous years. Additionally, air temperature during winter ranged from −29 °C to −10 °C in 2020 and −30 °C to −5 °C in 2021 (Figure 3b), the relatively higher E_n:E was thus related to a minimized effect of freezing and drought on the hydraulic functioning of *C. korshinskii* at the beginning of the growing season [23]. Meanwhile, the sharp increase in soil water availability in September promoted an increase in E_n and E_n:E, which was used to refill the embolized xylem conduits at the end of growing season. However, the seasonal trend of E_n:E_d in our study was contrary to that reported by Zhao et al. [38]. Relatively smaller differences between E_n and E_d from June to August during the growing season resulted from smaller differences in diurnal air temperature and T_{a-n} (Figure 3b).

4.3. Nocturnal Transpiration and Stem Refilling Dynamics of C. korshinskii

The partitioning of E_n into nocturnal transpiration (T_n) and stem refilling (R_e) is challenging because of their obvious temporal overlap. The forecasted refilling method has been successfully and widely used in previous studies on rain-free days under low levels of VPD_n. However, Chen et al. [22] indicated that E_n could also be influenced by nocturnal wind speeds, soil water content and their interaction. The accuracy of the forecasted refilling method can only be guaranteed under a low value of *VPD*. On every rain-free night in this study (Figures 2 and 3b), *VPD* was usually lower than that reported in *A. truncatum* [5] and *P. euphratica* [46]; we thus ignored the uncertainty of the forecasting method in this study. Our results indicate that, for *C. korshinskii*, T_n accounted for 49.76% and 54.44% of nocturnal water use, as the mean values of R_e:E_n throughout the growing season were 50.24% and 45.56% in 2020 and 2021, respectively. The R_e:E_n values were much higher than the 20%–25% observed for oak and pine growing in a humid montane region [27], and were similar to *S. superba* planted in a humid region in the dry season [20]; however, they were slightly lower than that found in *P. tomentosa* approximately 61% planted in a semiarid region [22], and much lower than that found in *P. euphratica* approximately 80% growing in an extremely arid environment [2] and *A. truncatum* (>85%) planted in an urban environment [5]. The higher value of R_e:E_n in the water-limited environment indicated a greater reliance of plants on the water stored through stem refilling, which could help forests to maintain hydraulic support under higher transpiration demand [47,48]. This might be why canopy transpiration in *C. korshinskii* remained steady during the middle

and end of the growing season (Figure listed in Zhang et al. [31]). Moreover, compared with that occurring in 2021, a relatively higher R_e:E_n (50.24%) value was observed in 2020, influenced by the relatively lower REW (Figures 3c and 5). Therefore, increasing R_e:E_n could be an important drought adaptation strategy for forests to overcome seasonal water stress in the growing season.

4.4. Environmental and Stomatal Effects on Nocturnal Water Use

We found that nocturnal water use usually fluctuated with changes in the site's environmental and stomatal variables. We found negative relationships between E_n and T_{a-n}, VPD_n and u_{2-n}, which was consistent with previous studies [12,23]. E_n was facilitated by VPD_n when light was absent, especially for young species. However, associated with an increased risk of xylem cavitation and decreased hydraulic conductance within plant tissue, stomatal closure was also triggered by low SWC and atmospheric drought [49,50]. An obvious response of the G_{c-n} threshold (1.5 mm s^{-1}) to E_n was observed in both 2020 and 2021 (Figure 6j). Variations in canopy stomatal conductance were proven to be strongly correlated with variations in site SWC and VPD [51]; nocturnal water use was thus significantly affected by soil drought, especially under high-VPD_n conditions. E_n then declined in the face of high transpiration demands during the night (Figure 6d). Therefore, the negative relationship between E_n and VPD_n might be related to the physiological effects of VPD_n on stomata [22]. E_n decreased exponentially with increasing u_{2-n} in this study, which was consistent with Gutiérrez et al. [52], but contrary to Zhao et al. [1]. The reasons for this could be as follows: (1) u_{2-n} underwent an obvious change at night during the growing season at our study site (Figure 3a), and (2) u_{2-n} mitigated T_{a-n} inversion and finally suppressed E_n by increasing VPD_n [53]. Soil water availability is an important variable controlling nocturnal water use according to previous studies [9,12]. However, REW had a weak influence on E_n in our study (Figure 7). Because soil water availability was very low surrounding the root system (Figure 3a), E_n and T_n were minimal when soil water content was low [21]. The response of T_n to VPD_n and G_{c-n} was similar to that of E_n, but different to that of R_e (Figure 6). A positive relationship between R_e and the VPD of previous day was reported for hybrid aspen coppice [6], indicating a high proportion of SF_n in the refilling of dehydrated tissues. However, the driving force of stem refilling became weak with the decrease in water demand [54], especially under high levels of VPD_n. The difference in the environmental and stomatal mechanisms between T_n and R_e dynamics might be related to disequilibrium between leaf and soil water potentials and the whole tree's hydraulic conductance [6]. Therefore, analysis of plant hydraulic capacity in planted forests should be undertaken in the future.

5. Conclusions

In this study, nocturnal water use dynamics and their environmental and stomatal control mechanism were explored for a *C. korshinskii* plantation on the Bashang Plateau. Nocturnal water use, transpiration and stem refilling in *C. korshinskii* accumulated to 14.36, 7.14 and 7.22 mm in 2020 and 14.51, 7.90 and 6.61 mm in 2021, respectively. Nocturnal transpiration accounted for 49.76% and 54.44% of total nocturnal water use, while stem refilling accounted for 50.24% and 45.56%, which indicates that *C. korshinskii* was able to draw on water stored in the stem to overcome seasonal drought. The sharp increase in the ratio of nocturnal to diurnal water use that appeared at the beginning and the end of the growing season might be an ecological strategy for recovering the hydraulic conductivity of the xylem conduits. Nocturnal water use was negatively correlated with all meteorological variables, but increased with increasing nocturnal canopy conductance, which indicates that nocturnal water use was sensitive to stomatal regulation at night. Specifically, nocturnal water use was predominantly affected by nocturnal canopy conductance, nocturnal air temperature and nocturnal wind speed. In contrast, canopy conductance, nocturnal air temperature, and nocturnal vapor pressure deficits explained the highest variation in nocturnal transpiration, and nocturnal vapor pressure deficits and nocturnal wind speed

explained the highest variation in stem refilling. The total effects of the five environmental and stomatal variables explained 50%, 36% and 32% of the nocturnal water use, nocturnal transpiration and stem refilling variation, respectively. Our results provide a new understanding of water use strategies employed by plants in *C. korshinskii* plantations on the Bashang Plateau, and suggest that ecophysiological responses and adaptation to increasing drought severity and duration will occur under future climate changes.

Author Contributions: Conceptualization, W.L.; methodology, W.L. and Y.Z.; investigation, N.W. and Z.Q.; data curation, B.X. and C.L.; Supervision, J.C. and Y.Y.; Writing—original draft, W.L.; Writing—review and editing, W.L. and Y.Z. All authors have read and agreed to the published version of the manuscript.

Funding: This research was funded by the National Natural Science Foundation of China (No. 42001027, 42101019, 42371048), Science and Technology Project of Hebei Education Department (BJK2022022), the Key Research and Development Plan Project of Hebei Province (22324202D), Natural Science Foundation of Hebei Province (D2021403023), the Key Research and Development Plan Project of Ningxia Hui Autonomous Region (2021BEG02008), Funding for the Science and Technology Innovation Team Project of Hebei GEO University (KJCXTD-2021-10), Innovation and Entrepreneurship Training Program for College Students (202210077015, S202210077021), and Hebei GEO University Student Science and Technology Fund (KAG202303).

Data Availability Statement: The data presented in this paper are available on request from the corresponding author.

Conflicts of Interest: The authors declare no conflict of interest.

Appendix A

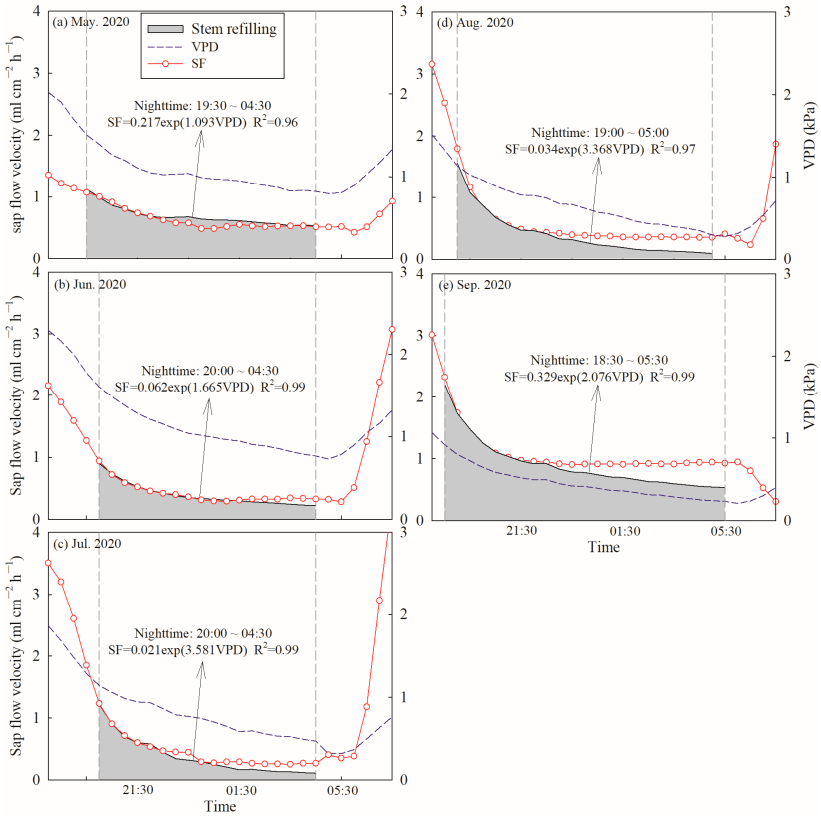

Figure A1. Examples of the forecasted refilling method used to determine the percentage of nocturnal sap flow velocity attributable to nocturnal transpiration and stem refilling in *C. korshinskii*. Nighttime was defined between dashed gray vertical lines (PAR < 5 μmol m^{-2} s^{-1}). Stem refilling is the shade proportion of nocturnal sap flow velocity, (**a**) May in 2020, (**b**) June in 2020, (**c**) July in 2020, (**d**) August in 2020 and (**e**) September in 2020.

References

1. Zhao, C.; Si, J.; Feng, Q.; Yu, T.; Li, P.; Forster, M.A. Nighttime transpiration of Populus euphratica during different phenophases. *J. For. Res.* **2019**, *30*, 435–444. [CrossRef]
2. Yu, T.; Feng, Q.; Si, J.; Mitchell, P.J.; Forster, M.A.; Zhang, X.; Zhao, C. Depressed hydraulic redistribution of roots more by stem refilling than by nocturnal transpiration for *Populus euphratica* Oliv. in situ measurement. *Ecol. Evol.* **2018**, *8*, 2607–2616. [CrossRef] [PubMed]
3. Dayer, S.; Herrera, J.C.; Dai, Z.; Burlett, R.; Lamarque, L.J.; Delzon, S.; Bortolami, G.; Cochard, H.; Gambetta, G.A. Nighttime transpiration represents a negligible part of water loss and does not increase the risk of water stress in grapevine. *Plant Cell Environ.* **2021**, *44*, 387–398. [CrossRef] [PubMed]
4. Siddiq, Z.; Cao, K.-F. Nocturnal transpiration in 18 broadleaf timber species under a tropical seasonal climate. *For. Ecol. Manag.* **2018**, *418*, 47–54. [CrossRef]
5. Wu, J.; Liu, H.; Zhu, J.; Gong, L.; Xu, L.; Jin, G.; Li, J.; Hauer, R.; Xu, C. Nocturnal sap flow is mainly caused by stem refilling rather than nocturnal transpiration for Acer truncatum in urban environment. *Urban Urban Gree.* **2020**, *56*, 126800. [CrossRef]
6. Kangur, O.; Tullus, A.; Sellin, A. Night-time transpiration, predawn hydraulic conductance and water potential disequilibrium in hybrid aspen coppice. *Trees* **2020**, *34*, 133–141. [CrossRef]
7. Zeppel, M.J.B.; Lewis, J.D.; Phillips, N.G.; Tissue, D.T. Consequences of nocturnal water loss: A synthesis of regulating factors and implications for capacitance, embolism and use in models. *Tree Physiol.* **2014**, *34*, 1047–1055. [CrossRef]
8. Dawson, T.E.; Burgess, S.S.O.; Tu, K.P.; Oliveira, R.S.; Santiago, L.S.; Fisher, J.B.; Simonin, K.A.; Ambrose, A.R. Nighttime transpiration in woody plants from contrasting ecosystems. *Tree Physiol.* **2007**, *27*, 561–575. [CrossRef]
9. Hayat, M.; Iqbal, S.; Zha, T.; Jia, X.; Qian, D.; Bourque, C.P.A.; Khan, A.; Tian, Y.; Bai, Y.; Liu, P.; et al. Biophysical control on nighttime sap flow in *Salix psammophila* in a semiarid shrubland ecosystem. *Agric. For. Meteorol.* **2021**, *300*, 108329. [CrossRef]
10. Lombardozzi, D.L.; Zeppel, M.J.B.; Fisher, R.A.; Tawfik, A. Representing nighttime and minimum conductance in CLM4.5: Global hydrology and carbon sensitivity analysis using observational constraints. *Geosci. Model. Dev.* **2017**, *10*, 321–331. [CrossRef]
11. Resco de Dios, V.; Chowdhury, F.I.; Granda, E.; Yao, Y.; Tissue, D.T. Assessing the potential functions of nocturnal stomatal conductance in C3 and C4 plants. *New Phytol.* **2019**, *223*, 1696–1706. [CrossRef]
12. Song, L.; Zhu, J.; Zheng, X.; Li, X.; Wang, K.; Zhang, J.; Wang, G.; Sun, H. Water use dynamics of trees in a Pinus tabuliformis plantation in semiarid sandy regions, Northeast China. *Agric. Water Manag.* **2023**, *275*, 107995. [CrossRef]
13. Phillips, N.G.; Lewis, J.D.; Logan, B.A.; Tissue, D.T. Inter- and intra-specific variation in nocturnal water transport in Eucalyptus. *Tree Physiol.* **2010**, *30*, 586–596. [CrossRef]
14. Zeppel, M.; Tissue, D.; Taylor, D.; Macinnis-Ng, C.; Eamus, D. Rates of nocturnal transpiration in two evergreen temperate woodland species with differing water-use strategies. *Tree Physiol.* **2010**, *30*, 988–1000. [CrossRef]
15. Zeppel, M.J.B.; Anderegg, W.R.L.; Adams, H.D.; Hudson, P.; Cook, A.; Rumman, R.; Eamus, D.; Tissue, D.T.; Pacala, S.W. Embolism recovery strategies and nocturnal water loss across species influenced by biogeographic origin. *Ecol. Evol.* **2019**, *9*, 5348–5361. [CrossRef] [PubMed]
16. de Dios, V.R.; Roy, J.; Ferrio, J.P.; Alday, J.G.; Landais, D.; Milcu, A.; Gessler, A. Processes driving nocturnal transpiration and implications for estimating land evapotranspiration. *Sci. Rep.* **2015**, *5*, 10975. [CrossRef]
17. Caspari, H.W.; Green, S.R.; Edwards, W.R.N. Transpiration of well-watered and water-stressed Asian pear trees as determined by lysimetry, heat-pulse, and estimated by a Penman-Monteith model. *Agric. For. Meteorol.* **1993**, *67*, 13–27. [CrossRef]
18. Buckley, T.N.; Turnbull, T.L.; Pfautsch, S.; Adams, M.A. Nocturnal water loss in mature subalpine *Eucalyptus delegatensis* tall open forests and adjacent *E. pauciflora* woodlands. *Ecol. Evol.* **2011**, *1*, 435–450. [CrossRef] [PubMed]
19. Ford, C.R.; Goranson, C.E.; Mitchell, R.J.; Will, R.E.; Teskey, R.O. Modeling canopy transpiration using time series analysis: A case study illustrating the effect of soil moisture deficit on *Pinus taeda*. *Agric. For. Meteorol.* **2005**, *130*, 163–175. [CrossRef]
20. Zhao, X.; Zhao, P.; Zhu, L. Differentiating refilling and transpiration from night-time sap flux based on time series modelling. *Trees* **2022**, *36*, 1621–1632. [CrossRef]
21. Fisher, J.B.; Baldocchi, D.D.; Misson, L.; Dawson, T.E.; Goldstein, A.H. What the towers don't see at night: Nocturnal sap flow in trees and shrubs at two AmeriFlux sites in California. *Tree Physiol.* **2007**, *27*, 597–610. [CrossRef] [PubMed]
22. Chen, Z.; Zhang, Z.; Sun, G.; Chen, L.; Xu, H.; Chen, S. Biophysical controls on nocturnal sap flow in plantation forests in a semi-arid region of northern China. *Agric. For. Meteorol.* **2020**, *284*, 107904. [CrossRef]
23. Di, N.; Xi, B.; Clothier, B.; Wang, Y.; Li, G.; Jia, L. Diurnal and nocturnal transpiration behaviors and their responses to groundwater-table fluctuations and meteorological factors of *Populus tomentosa* in the North China Plain. *For. Ecol. Manag.* **2019**, *448*, 445–456. [CrossRef]
24. Chu, C.R.; Hsieh, C.-I.; Wu, S.-Y.; Phillips, N.G. Transient response of sap flow to wind speed. *J. Exp. Bot.* **2009**, *60*, 249–255. [CrossRef]
25. Si, J.; Feng, Q.; Yu, T.; Zhao, C. Nighttime sap flow and its driving forces for *Populus euphratica* in a desert riparian forest, Northwest China. *J. Arid. Land* **2015**, *7*, 665–674. [CrossRef]

26. Fuentes, S.; Mahadevan, M.; Bonada, M.; Skewes, M.A.; Cox, J.W. Night-time sap flow is parabolically linked to midday water potential for field-grown almond trees. *Irrig. Sci.* **2013**, *31*, 1265–1276. [CrossRef]
27. Alvarado-Barrientos, M.S.; Holwerda, F.; Geissert, D.R.; Muñoz-Villers, L.E.; Gotsch, S.G.; Asbjornsen, H.; Dawson, T.E. Nighttime transpiration in a seasonally dry tropical montane cloud forest environment. *Trees* **2015**, *29*, 259–274. [CrossRef]
28. Fang, W.; Lu, N.; Liu, J.; Jiao, L.; Zhang, Y.; Wang, M.; Fu, B. Canopy transpiration and stand water balance between two contrasting hydrological years in three typical shrub communities on the semiarid Loess Plateau of China. *Ecohydrology* **2019**, *12*, e2064. [CrossRef]
29. Jian, S.; Zhao, C.; Fang, S.; Yu, K. Effects of different vegetation restoration on soil water storage and water balance in the Chinese Loess Plateau. *Agric. For. Meteorol.* **2015**, *206*, 85–96. [CrossRef]
30. Li, B.-B.; Li, P.-P.; Zhang, W.-T.; Ji, J.-Y.; Liu, G.-B.; Xu, M.-X. Deep soil moisture limits the sustainable vegetation restoration in arid and semi-arid Loess Plateau. *Geoderma* **2021**, *399*, 115122. [CrossRef]
31. Zhang, Y.; Li, W.; Yan, H.; Xie, B.; Zhao, J.; Wang, N.; Wang, X. Canopy Transpiration and Stomatal Conductance Dynamics of *Ulmus pumila* L. and *Caragana korshinskii* Kom. Plantations on the Bashang Plateau, China. *Forests* **2022**, *13*, 1081. [CrossRef]
32. Campbell, G.S.; Norman, J.M. *An Introduction to Environmental Biophysics*; Springer Science & Business Media: Berlin/Heidelberg, Germany, 2000.
33. Lubczynski, M.W.; Chavarro-Rincon, D.; Roy, J. Novel, cyclic heat dissipation method for the correction of natural temperature gradients in sap flow measurements. Part 1. Theory and application. *Tree Physiol.* **2012**, *32*, 894–912. [CrossRef]
34. Granier, A. Evaluation of transpiration in a Douglas-fir stand by means of sap flow measurements. *Tree Physiol.* **1987**, *3*, 309–320. [CrossRef] [PubMed]
35. Lu, P.; Urban, L.; Zhao, P. Granier's thermal dissipation probe (TDP) method for measuring sap flow in trees: Theory and practice. *Acta Bot. Sin.* **2004**, *46*, 631–646.
36. Rabbel, I.; Diekkrüger, B.; Voigt, H.; Neuwirth, B. Comparing ΔTmax Determination Approaches for Granier-Based Sapflow Estimations. *Sensors* **2016**, *16*, 2042. [CrossRef] [PubMed]
37. Song, L.; Zhu, J.; Zhang, T.; Wang, K.; Wang, G.; Liu, J. Higher canopy transpiration rates induced dieback in poplar (Populus × xiaozhuanica) plantations in a semiarid sandy region of Northeast China. *Agric. Water Manag.* **2021**, *243*, 106414. [CrossRef]
38. Zhao, C.Y.; Si, J.H.; Feng, Q.; Yu, T.F.; Li, P.D. Comparative study of daytime and nighttime sap flow of Populus euphratica. *Plant Growth Regul.* **2017**, *82*, 353–362. [CrossRef]
39. Igarashi, Y.; Kumagai, T.o.; Yoshifuji, N.; Sato, T.; Tanaka, N.; Tanaka, K.; Suzuki, M.; Tantasirin, C. Environmental control of canopy stomatal conductance in a tropical deciduous forest in northern Thailand. *Agric. For. Meteorol.* **2015**, *202*, 1–10. [CrossRef]
40. Mei, T.; Fang, D.; Röll, A.; Niu, F.; Hendrayanto; Hölscher, D. Water Use Patterns of Four Tropical Bamboo Species Assessed with Sap Flux Measurements. *Front. Plant Sci.* **2016**, *6*, 1202. [CrossRef]
41. Zeng, X.; Xu, X.; Yi, R.; Zhong, F.; Zhang, Y. Sap flow and plant water sources for typical vegetation in a subtropical humid karst area of southwest China. *Hydrol. Process.* **2021**, *35*, e14090. [CrossRef]
42. Wu, S.; Gu, X.; Zheng, Y.; Chen, L. Nocturnal sap flow as compensation for water deficits: An implicit water-saving strategy used by mangroves in stressful environments. *Front. Plant Sci.* **2023**, *14*, 1118970. [CrossRef] [PubMed]
43. Xiu, Z.-H.; Ping, Z.; Zhen, Z.-Z.; Li, Z.-W.; Jun, N.-F.; Guang, N.-Y.; Yan, H.-T.; Lei, O. Sap flow-based transpiration in Phyllostachys pubescens: Applicability of the TDP methodology, age effect and rhizome role. *Trees* **2017**, *31*, 765–779. [CrossRef]
44. Xie, J.; Wan, X. The accuracy of the thermal dissipation technique for estimating sap flow is affected by the radial distribution of conduit diameter and density. *Acta Physiol. Plant.* **2018**, *40*, 88. [CrossRef]
45. Hölttä, T.; Dominguez Carrasco, M.D.R.; Salmon, Y.; Aalto, J.; Vanhatalo, A.; Bäck, J.; Lintunen, A. Water relations in silver birch during springtime: How is sap pressurised? *Plant Biol.* **2018**, *20*, 834–847. [CrossRef] [PubMed]
46. Yu, T.; Feng, Q.; Si, J.; Pinkard, E.A. Coordination of stomatal control and stem water storage on plant water use in desert riparian trees. *Trees* **2019**, *33*, 787–801. [CrossRef]
47. McCulloh, K.A.; Johnson, D.M.; Meinzer, F.C.; Woodruff, D.R. The dynamic pipeline: Hydraulic capacitance and xylem hydraulic safety in four tall conifer species. *Plant Cell Environ.* **2014**, *37*, 1171–1183. [CrossRef]
48. Yi, K.; Dragoni, D.; Phillips, R.P.; Roman, D.T.; Novick, K.A. Dynamics of stem water uptake among isohydric and anisohydric species experiencing a severe drought. *Tree Physiol.* **2017**, *37*, 1379–1392. [CrossRef]
49. Cirelli, D.; Equiza, M.A.; Lieffers, V.J.; Tyree, M.T. Populus species from diverse habitats maintain high night-time conductance under drought. *Tree Physiol.* **2016**, *36*, 229–242. [CrossRef]
50. Shen, Q.; Gao, G.; Fu, B.; Lü, Y. Responses of shelterbelt stand transpiration to drought and groundwater variations in an arid inland river basin of Northwest China. *J. Hydrol.* **2015**, *531*, 738–748. [CrossRef]
51. Zha, T.; Barr, A.G.; van der Kamp, G.; Black, T.A.; McCaughey, J.H.; Flanagan, L.B. Interannual variation of evapotranspiration from forest and grassland ecosystems in western canada in relation to drought. *Agric. For. Meteorol.* **2010**, *150*, 1476–1484. [CrossRef]
52. GutiÉRrez, M.V.; Meinzer, F.C.; Grantz, D.A. Regulation of transpiration in coffee hedgerows: Covariation of environmental variables and apparent responses of stomata to wind and humidity. *Plant Cell Environ.* **1994**, *17*, 1305–1313. [CrossRef]

53. Green, S.R.; McNaughton, K.G.; Clothier, B.E. Observations of night-time water use in kiwifruit vines and apple trees. *Agric. For. Meteorol.* **1989**, *48*, 251–261. [CrossRef]
54. Karpul, R.H.; West, A.G. Wind drives nocturnal, but not diurnal, transpiration in Leucospermum conocarpodendron trees: Implications for stilling on the Cape Peninsula. *Tree Physiol.* **2016**, *36*, 954–966. [CrossRef] [PubMed]